

The First Dynamical Mass Measurement in the HR 8799 System

G. MIREK BRANDT ^{1,*} TIMOTHY D. BRANDT ¹ TRENT J. DUPUY ² DANIEL MICHALIK ³ AND
GABRIEL-DOMINIQUE MARLEAU ^{4,5,6}

¹*Department of Physics, University of California, Santa Barbara, Santa Barbara, CA 93106, USA*

²*Institute for Astronomy, University of Edinburgh, Royal Observatory, Blackford Hill, Edinburgh, EH9 3HJ, UK*

³*European Space Agency (ESA), European Space Research and Technology Centre (ESTEC), Keplerlaan 1, 2201 AZ Noordwijk, The Netherlands*

⁴*Institut für Astronomie und Astrophysik, Universität Tübingen, Auf der Morgenstelle 10, 72076 Tübingen, Germany*

⁵*Physikalisches Institut, Universität Bern, Gesellschaftsstr. 6, 3012 Bern, Switzerland*

⁶*Max-Planck-Institut für Astronomie, Königstuhl 17, 69117 Heidelberg, Germany*

(Received April 7, 2021; Revised May 14, 2021; Accepted May 26, 2021)

Submitted to ApJ Letters

ABSTRACT

HR 8799 hosts four directly imaged giant planets, but none has a mass measured from first principles. We present the first dynamical mass measurement in this planetary system, finding that the innermost planet HR 8799 e has a mass of $9.6_{-1.8}^{+1.9} M_{\text{Jup}}$. This mass results from combining the well-characterized orbits of all four planets with a new astrometric acceleration detection (5σ) from the *Gaia* EDR3 version of the *Hipparcos-Gaia* Catalog of Accelerations. We find with 95% confidence that HR 8799 e is below $13 M_{\text{Jup}}$, the deuterium-fusing mass limit. We derive a hot-start cooling age of 42_{-16}^{+24} Myr for HR 8799 e that agrees well with its hypothesized membership in the Columba association but is also consistent with an alternative suggested membership in the β Pictoris moving group. We exclude the presence of any additional $\gtrsim 5 M_{\text{Jup}}$ planets interior to HR 8799 e with semi-major axes between ≈ 3 –16 au. We provide proper motion anomalies and a matrix equation to solve for the mass of any of the planets of HR 8799 using only mass ratios between the planets.

Keywords: —

1. INTRODUCTION

HR 8799 is the only star that has been detected with four directly imaged exoplanets (Marois et al. 2008; Marois et al. 2010; Currie et al. 2011). Each planet orbits counter-clockwise on the sky, in a gently eccentric orbit, with a nearly face-on configuration (Sudol & Haghighipour 2012; Pueyo et al. 2015; Konopacky et al. 2016; Currie 2016). The orbits of all four planets are known with exquisite precision. Wang et al. (2018) studied the system in detail and restricted orbital parameter space based on configurations that are dynamically stable. There have been many mass constraints based on the long term dynamical stability of the system (e.g., all planets $\lesssim 5 M_{\text{Jup}}$ by Esposito et al. 2013; inner three planets $< 13 M_{\text{Jup}}$ by Pueyo et al. 2015). However, there are no robust dynamical, i.e., from Newtonian mechan-

ics, mass measurements for any of the planets in the HR 8799 system.

The HR 8799 planets induce accelerations on their host star that are measurable by sufficiently precise absolute astrometry, enabling direct, dynamical measurements of the planets’ masses. The *Hipparcos-Gaia* catalog of accelerations (HGCA, Brandt 2018, 2021) has cross-calibrated the positions and proper motions so that these accelerations can be used for inference. The acceleration of HR 8799 A was not significant in the *Gaia* DR2 (Lindgren et al. 2018) version of the catalog (Brandt 2018). However, *Gaia*’s precision on bright stars has increased significantly in EDR3 (Gaia Collaboration et al. 2020; Lindgren et al. 2020; Brandt 2021). In the *Gaia* EDR3 version of the HGCA, HR 8799 A is accelerating at nearly 5σ . In this paper we infer the mass, and thereafter the age, of HR 8799 e from this acceleration.

* NSF Graduate Research Fellow

The HR 8799 system is most commonly thought to be an ≈ 40 -Myr-old member of the Columba association (Zuckerman et al. 2011), but Lee & Song (2019) recently suggested membership with the younger β Pic Moving Group (BPMG). Given a ≈ 40 -Myr age, hot-start evolutionary models predict masses of $7 \pm 2 M_{\text{Jup}}$ for the innermost three planets, well below the deuterium-fusion mass boundary ($\approx 12\text{--}13 M_{\text{Jup}}$; Spiegel et al. 2011). Lower masses ($\lesssim 5\text{--}7 M_{\text{Jup}}$) improve the system’s dynamical stability (Fabrycky & Murray-Clay 2010; Sudol & Haghighipour 2012), but resonant locking could render the system stable at higher planet masses (Götberg et al. 2016; Wang et al. 2018; Goździewski & Migaszewski 2018, 2020). Higher masses would imply either an older age for the system or entropy loss during formation (a colder start), although there is a limit to the entropy that can be lost at formation (Marleau & Cumming 2014). Conversely, lower masses would suggest a younger age and therefore favor membership with the BPMG. Dynamical mass measurements can conclusively test such hypotheses. The inferred atmospheric properties and chemical abundances of the planets also depend on their assumed masses (e.g., Wang et al. 2020; Mollière et al. 2020).

We detail our method in Section 2. In Section 3 we consider planet mass ratios estimated from their relative luminosities, show that the mass of HR 8799 e is insensitive to these mass ratios, and obtain a robust dynamical mass measurement. We derive a substellar cooling age for HR 8799 e in Section 4 and conclude in Section 5.

2. METHODOLOGY

The acceleration that HR 8799 A experiences is the sum of the acceleration due to each of its four planetary companions. Because the planet masses are small compared to the mass of HR 8799 A ($1.47_{-0.08}^{+0.11} M_{\odot}$; Wang et al. 2018), the star’s motion is approximately given by a linear combination of the orbits of the planets, weighted by their masses. We can then optimize the planet masses until the modelled host star acceleration matches the observed value.

We use all 1000 samples from the orbital posteriors from Wang et al. (2018), published on the github repository for the resource whereistheplanet.com (Wang et al. 2021). The orbits correspond to the coplanar, dynamically stable case of the HR 8799 system (see Table 4 of Wang et al. 2018). Each set of orbital parameters, together with the masses of the four planets and the star, predicts the motion of HR 8799 A.

Wang et al. (2018) used the *Gaia* DR1 parallax of 24.76 ± 0.64 mas (Gaia Collaboration et al. 2016)¹. *Gaia* EDR3 measures a much more precise value of 24.462 ± 0.046 mas (Lindegren et al. 2020). We scale all 1000 MCMC samples to the *Gaia* EDR3 parallax, removing its contribution to the uncertainty of the orbital fits. Defining r to be the ratio of a given chain’s parallax to the *Gaia* EDR3 value, we multiply the semi-major axes by r (to preserve the relative astrometry) and multiply the system mass by r^3 (to preserve the orbital periods). We keep all other orbital parameters unchanged. Updating the parallax to its *Gaia* EDR3 value ultimately improves the fractional error on the final mass estimate from 20% to 19.5%.

We use the open-source tool `htof` (Brandt et al. 2020, submitted; Brandt & Michalik 2020; Brandt et al. 2021b) to model *Hipparcos* and *Gaia* observations. In brief, `htof` uses the *Hipparcos* intermediate astrometric data (both ESA (1997) and van Leeuwen (2007) reductions) and predicted scan angles and observational epochs of *Gaia* (via GOST²), to generate synthetic *Hipparcos* and *Gaia* astrometry for any orbit.

The astrometric measurement that we use is the proper motion anomaly. This is the difference between a nearly instantaneous proper motion from *Gaia* EDR3 and a long-term proper motion (the difference in position between the *Hipparcos* and *Gaia* astrometry missions divided by the time between the measurements). We denote these proper motion anomalies as, e.g.,

$$\Delta\mu_{\alpha*} = \mu_{\text{Gaia}} - \frac{\alpha^*_{\text{Gaia}} - \alpha^*_{\text{Hip}}}{t_{\text{Gaia}} - t_{\text{Hip}}} \quad (1)$$

where $\alpha^* = \alpha \cos \delta$. Parameters with subscript *Hip* refers to the average of those parameters from *Hipparcos* 2007 and 1997, weighted 60/40 as they are in the HGCA (Brandt 2018). A set of orbital parameters then gives predicted values for $\Delta\mu_{\alpha*}$ and $\Delta\mu_{\delta}$ as functions of the masses of the planets, m_b, m_c, m_d , and m_e . Because HR 8799 A’s motion closely follows a linear combination of Keplerian orbits, we can represent its predicted proper motion anomaly as the Jacobian

$$\begin{bmatrix} \Delta\mu_{\alpha*} \\ \Delta\mu_{\delta} \end{bmatrix}_{\text{model}} = \begin{bmatrix} \frac{\partial\Delta\mu_{\alpha*}}{\partial m_b} & \frac{\partial\Delta\mu_{\alpha*}}{\partial m_c} & \frac{\partial\Delta\mu_{\alpha*}}{\partial m_d} & \frac{\partial\Delta\mu_{\alpha*}}{\partial m_e} \\ \frac{\partial\Delta\mu_{\delta}}{\partial m_b} & \frac{\partial\Delta\mu_{\delta}}{\partial m_c} & \frac{\partial\Delta\mu_{\delta}}{\partial m_d} & \frac{\partial\Delta\mu_{\delta}}{\partial m_e} \end{bmatrix} \begin{bmatrix} m_b \\ m_c \\ m_d \\ m_e \end{bmatrix}. \quad (2)$$

¹ In all cases where we quote a posterior by listing m_{-l}^{+u} or $m \pm \sigma$: m denotes the median with l and u (or singularly, σ) denoting the 16% and 84% confidence intervals, respectively.

² <https://gaia.esac.esa.int/gost/>

We compute the partial derivatives by using only the orbit of a given planet and assigning that planet unit mass. We do this for all 1000 orbital draws. We use REBOUND and the `ias15` scheme (Rein & Liu 2012; Rein & Spiegel 2015) to integrate the orbits in time.

When we compute the model partial derivatives, we mix the ESA (1997) and van Leeuwen (2007) positions according to the same 60/40 ratio adopted by the HGCA. Brandt (2018) show in their Section 7 and Figure 2 that a 60/40 mix of the two *Hipparcos* reductions’ proper motion measurements better matches the long-term proper motions between *Hipparcos* and *Gaia* than either reduction on its own. The EDR3 version of the HGCA (Brandt 2021) confirms this finding and also shows that a 60/40 mix of the two *Hipparcos* reductions’ position measurements best matches the *Gaia* positions extrapolated back to the *Hipparcos* observational epoch. We compute our positions at the same central epochs as given in the HGCA³. This forward modeling allows us to directly compare our proper motion anomalies to the values given in the HGCA. The HGCA is calibrated so that the measured proper motion anomalies have Gaussian uncertainties. We can therefore identify χ^2 with $-2\ln\mathcal{L}$ and find the masses by maximizing the likelihood \mathcal{L} , or minimizing

$$\chi^2 = -2\ln\mathcal{L} = \mathbf{d}^T (\mathbf{C}_{HG} + \mathbf{C}_{Gaia})^{-1} \mathbf{d} \quad (3)$$

where \mathbf{C}_{HG} is the HGCA covariance matrix for the two *Hipparcos*-*Gaia* long-term proper motions, \mathbf{C}_{Gaia} is the HGCA covariance matrix for the two *Gaia* EDR3 proper motions, and

$$\mathbf{d} = \begin{bmatrix} \Delta\mu_{\alpha*model} - \Delta\mu_{\alpha*HGCA} \\ \Delta\mu_{\delta model} - \Delta\mu_{\delta HGCA} \end{bmatrix}. \quad (4)$$

In Equation (4), $\Delta\mu_{\alpha*model}$ and $\Delta\mu_{\delta model}$ are calculated from the right-hand side of Equation 2. \mathbf{C}_{HG} and \mathbf{C}_{Gaia} are given in the HGCA. We republish their sum here, along with the anomalies, for ease of reproducibility:

$$\mathbf{C}_{HG} + \mathbf{C}_{Gaia} = \begin{bmatrix} 6.5934 & 0.7473 \\ 0.7473 & 6.9888 \end{bmatrix} 10^{-3} (\text{mas yr}^{-1})^2 \quad (5)$$

$$\begin{bmatrix} \Delta\mu_{\alpha*HGCA} \\ \Delta\mu_{\delta HGCA} \end{bmatrix} = \begin{bmatrix} -0.268 \\ -0.348 \end{bmatrix} \text{mas yr}^{-1}. \quad (6)$$

³ These central epochs are, in years for dec. and right-ascension: 2015.85 2015.76 for *Gaia* EDR3 and 1991.35 1991.34 for *Hipparcos*.

We compute the partial derivatives of Equation (3) against $\Delta\mu_{\alpha*}$, and $\Delta\mu_{\delta}$. Setting these partials to zero gives an under-constrained system of equations. The two components of the proper motion anomaly measure a combination of the masses of the four planets, but not the four masses individually. However, if we assume a relationship between the individual masses, then Equation (3) produces an over-constrained system for the masses. If we take a uniform prior on one planet mass and assume mass ratios for the remaining three planets, Equation (3) represents a Gaussian mass posterior for each set of orbital parameters.

3. RESULTS

In this section we use Equations (2)–(6), together with varying assumptions about the mass ratios of the four planets, to derive constraints on the mass of HR 8799 e.

3.1. Fixed mass ratios

We initially assume the fixed mass ratios derived by Wang et al. (2018) from the observed luminosities assuming hot-start models,

$$m_e = m_d = m_c = 1.25m_b. \quad (7)$$

With the assumed ratios of the masses of the four planets, Equation (3) fits one free parameter to two covariant data points. We begin with the calculation of the Jacobians, Equation (2) (one for each of the 1000 orbital draws). We fit 1000 Jacobians and sum the posteriors. The resulting posterior is very nearly Gaussian with mean $9.59M_{\text{Jup}}$ and standard deviation $1.84M_{\text{Jup}}$. The residual from the best-fit mass should be χ^2 -distributed with one degree of freedom. The best-fit χ^2 is only 0.05: the observed astrometric acceleration from the HGCA agrees almost perfectly with the model prediction using the Wang et al. (2018) orbits and mass ratios.

Because the orbital elements of the HR 8799 planets are so well characterized, the derivatives of the anomalies with respect to each planet’s mass vary little between the MCMC draws. The element-wise median Jacobian matrix is an approximation to all 1000 sets of orbital parameters; it is given by

$$\frac{\mathbf{J}_{\text{median}}}{\text{mas yr}^{-1} M_{\text{Jup}}^{-1}} = \begin{bmatrix} 2.00 & -3.94 & -3.01 & -24.20 \\ 1.14 & 3.80 & -13.74 & -26.05 \end{bmatrix}. \quad (8)$$

The width of our posterior is dominated by the observational uncertainty in absolute astrometry from the HGCA, which corresponds to about $\pm 1.8M_{\text{Jup}}$ (20%). The uncertainty in the mass of HR 8799 e from the orbital draws alone is just $0.35M_{\text{Jup}}$ (enlarging the final

error bars by only 2%). Using the median Jacobian (Equation (8)) together with the mass ratios in Equation (7), and broadening with the orbital motion uncertainty ($0.35 M_{\text{Jup}}$), gives a posterior that is indistinguishable from the full posterior using 1000 sets of orbital parameters.

We use the median Jacobian matrix for the remainder of this work and convolve our posterior mass distributions for HR 8799 e with a Gaussian of standard deviation $0.35 M_{\text{Jup}}$ (which accounts for the negligible contribution from orbital motion uncertainty).

3.2. Varying mass ratios

The mass ratios of the four planets are known only to roughly $\pm 15\%$ from hot-start models (Wang et al. 2018). We now show that the mass of HR 8799 e is robust to larger variations in the mass ratios. We quantify changes in the mass ratios by three coefficients γ_i , which we define by

$$m_e = \gamma_d m_d = \gamma_c m_c = \gamma_b 1.25 m_b. \quad (9)$$

Setting $\gamma_d = \gamma_c = \gamma_b = 1$ yields the fiducial mass ratios.

Figure 1 shows the mass posterior of HR 8799 e assuming nine different mass ratios. We vary each of the γ_i independently between 0.7 to 1.4 (corresponding to varying the masses of b, c, and d by roughly $\pm 4 M_{\text{Jup}}$). Varying the mass ratio of planet b or c to planet e by this amount changes the inferred mass of HR 8799 e by $\lesssim 0.1 M_{\text{Jup}}$, or $\lesssim 0.05\sigma$. The top curves in Figure 1 show that the mass of HR 8799 e is covariant with HR 8799 d but that the variation is $\approx 1 M_{\text{Jup}}$, or $\approx 0.5\sigma$, even with the extreme range of mass ratios presented. Taylor expanding the maximum likelihood mass, $\langle m_e \rangle$, about our base case mass ratios $\gamma_d = \gamma_c = \gamma_b = 1$ yields

$$\frac{\langle m_e \rangle}{M_{\text{Jup}}} \approx 9.56 - 2.50(\gamma_d - 1) - 0.001(\gamma_c - 1) + 0.37(\gamma_b - 1). \quad (10)$$

The mass of HR 8799 d is moderately covariant with that of HR 8799 e, while HR 8799 b and HR 8799 c have little effect: b is too far away, while c induces a proper motion anomaly nearly perpendicular to that induced by e.

We now generalize Figure 1 by marginalizing over the possible range of mass ratios (i.e., effectively summing the posteriors of Figure 1). We use independent, log-normal priors (base- e lognormal) centered on unity for each of γ_d , γ_c , and γ_b . For our fiducial case, we take the γ_i priors to have standard deviation 0.15 of the natural logarithm (0.065 dex). This corresponds to $\pm 15\%$, reflecting hot-start uncertainties (Wang et al. 2018). We

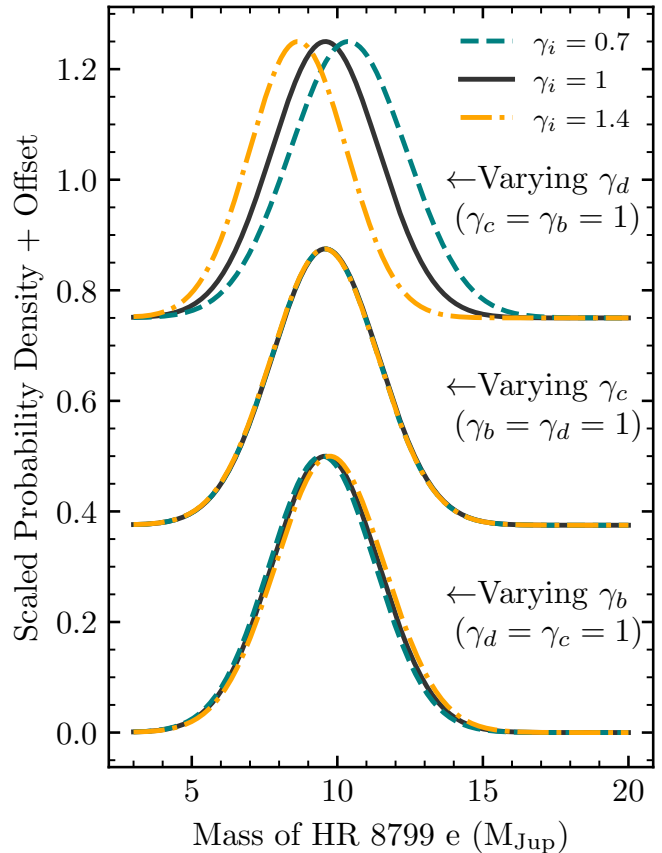


Figure 1. Posteriors for the mass of HR 8799 e, varying the assumed mass ratio of each other planet relative to planet e from 70% ($\gamma = 0.7$, teal dashed lines) to 140% ($\gamma = 1.4$, orange dot-dashed lines) of its fiducial value (see Equation (9)). The mass of HR 8799 e is moderately covariant with that of planet d but insensitive to the masses of planets b and c.

also include a worst-case where we use a logarithmic prior with a standard deviation of 0.45 (0.2 dex). This allows for deviations in the mass ratios of roughly -35% and $+55\%$, slightly more than that shown in Figure 1.

Figure 2 shows the posteriors on planet e’s mass under the two prior choices. Our preferred result is a nearly Gaussian posterior of $9.6^{+1.9}_{-1.8} M_{\text{Jup}}$. Adopting our worst-case prior, allowing for three times the range of mass ratios, yields $9.4^{+2.2}_{-2.1} M_{\text{Jup}}$.

3.3. Additional companions

An additional companion is detectable if it causes a significant astrometric perturbation on the host star. Figure 3 shows the semi-major axes and masses that an additional, unseen massive companion would need to cause perturbation large enough to be detected in *Gaia* EDR3. Planets in the blue region above the grey band would have yielded a significant (3σ) astrometric acceleration on the system that we would have seen in our

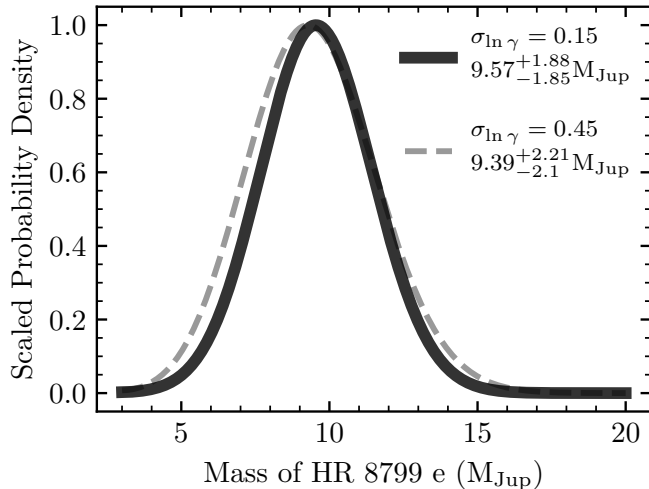


Figure 2. The mass posterior of HR 8799 e after marginalizing over bcd-to-e mass ratios (quantified by three γ_i coefficients), each with a lognormal prior. Each posterior is labelled according to both its mass-ratio prior and the resulting posterior (non-rounded for convenience). $\sigma_{\ln \gamma}$ is the natural logarithmic standard deviation of the log-normal prior on the γ_i . Each prior has a natural logarithmic mean of 0.

analysis. Additional planets in the parameter space below the grey band (white region) are not excluded. We conclude that additional, unseen massive planets orbiting between 3 and 8 au with masses exceeding $6 M_{\text{Jup}}$ are unlikely, as well as $\gtrsim 7 M_{\text{Jup}}$ companions between 8 au and the orbit of HR 8799 e (≈ 16 au). We therefore exclude the presence of any $\gtrsim 7 M_{\text{Jup}}$ companions orbiting amidst the inner debris belt, which spans 6–15 au (Frantseva et al. 2020). Our detection limits complement the findings by Wahhaj et al. (2021), who excluded the presence of hot-start planets more massive than $\gtrsim 3 M_{\text{Jup}}$ at two separations: 7.5 and 9.7 au.

4. THE AGE OF THE HR 8799 SYSTEM

With our dynamical mass for HR 8799 e, we infer the first cooling age for the planet and thereby the system. Prior to Zuckerman et al. (2011) identifying it as a member of the Columba association (42^{+6}_{-4} Myr; Bell et al. 2015), its age was only loosely constrained (Marois et al. 2008). Lee & Song (2019) recently suggested that it is actually a member of the younger β Pictoris moving group (BPMG, 24 ± 3 Myr; Bell et al. 2015). Moreover, HR 8799 was one of four (out of 23) Columba members that Gagné et al. (2018) chose not to use in their BANYAN Σ model due to being outliers, despite it still being considered a bona fide member.

We perform a rejection-sampling analysis using mass and L_{bol} , in a similar fashion as Dupuy & Liu (2017) and Brandt et al. (2021, submitted), to derive a hot-start cooling age for HR 8799 e. The HR 8799 planets are

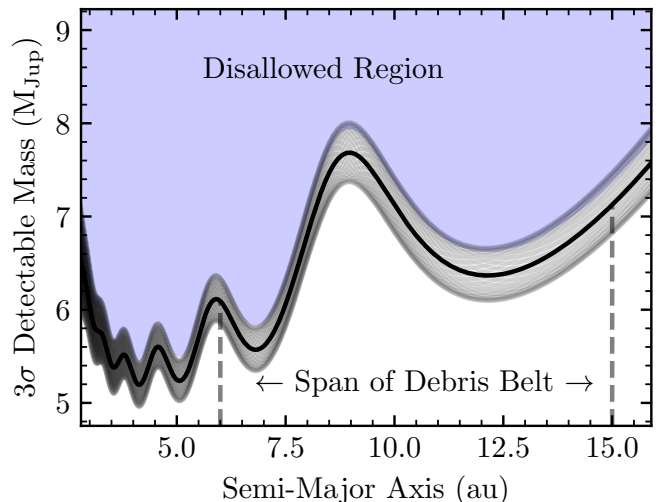


Figure 3. The minimum masses and semi-major axes of additional, unseen HR 8799 companions that would have been detected at 3σ using our HGCA *Gaia* EDR3-*Hipparcos* proper motion anomalies. The individual grey lines (forming a grey band together) show the 3σ limits assuming a range of argument of periastron (ω) from 0 to 2π . The black line is the 3σ limit averaged over the all possible ω . Planets lying in the blue “disallowed region” are excluded with at least 99.7% confidence, regardless of their orbital phase. The approximate range of the inner debris belt is indicated by vertical dashed lines (6 to 15 au; Frantseva et al. 2020).

too luminous to be consistent with the very low initial entropies predicted by the Marley et al. (2007) cold-start models (Marleau & Cumming 2014). Warm- and hot-start scenarios are allowed by the data, and simulations from Berardo et al. (2017), Berardo & Cumming (2017), and Marleau et al. (2019) tend to favor the hot-start scenario in general.

We randomly draw masses from our posterior distribution and ages distributed uniformly or log-flat, then bi-linearly interpolate the evolutionary model grid and compute a test L_{bol} . We accept or reject trials in a Monte Carlo fashion depending on how well the trials agree with the observed L_{bol} .

We derive a new L_{bol} for HR 8799 e using the absolute magnitude- L_{bol} relations of Dupuy & Liu (2017), the SPHERE photometry from Wahhaj et al. (2021), and the K -band spectrum from Gravity Collaboration et al. (2019). Although the relations of Dupuy & Liu (2017) are derived from field dwarfs, Figure 12 of Filippazzo et al. (2015) demonstrates that young and field objects share the same K -band bolometric corrections within the 0.25 mag scatter of their relations; we adopt this scatter as our uncertainty. We find $K_{\text{MKO}} = K_{\text{S,2MASS}} = 16.00 \pm 0.02$ mag and $\log(L_{\text{bol}}/L_{\odot}) = -4.52 \pm 0.10$ dex, which is consistent with but twice as precise as the measurement by Marois et al. (2010).

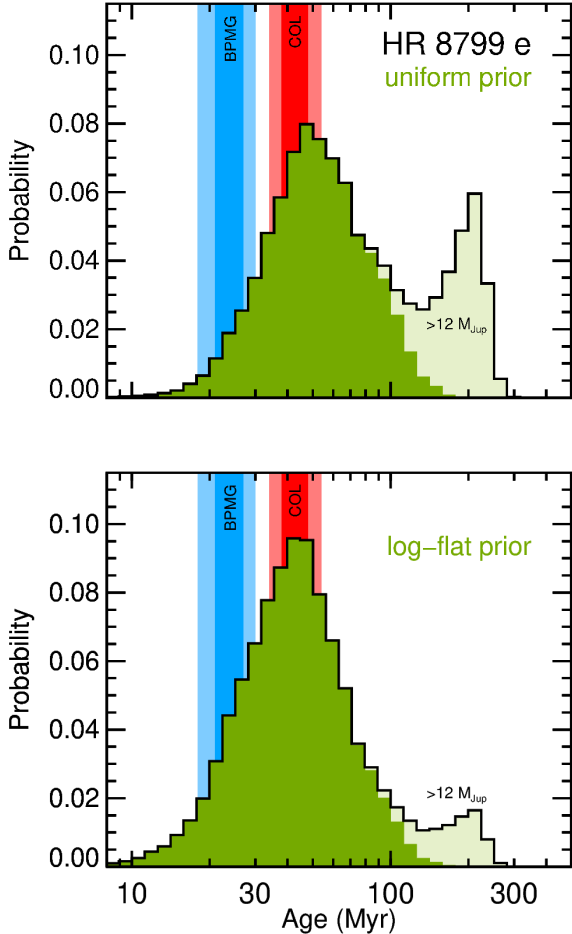


Figure 4. Substellar cooling age for HR 8799 e derived from hot-start Saumon & Marley (2008) hybrid models using its observed luminosity and dynamical mass, with either a uniform (top panel) or log-flat (bottom panel) prior on age. The 1σ and 2σ age ranges for the Columba association (red) and the BPMG (blue) are displayed for comparison, and our cooling age is consistent with both. The peak at ≈ 200 Myr corresponds to the 10% of our mass posterior above $12 M_{\text{Jup}}$ (lighter shading). The maximum likelihood age is 40–50 Myr regardless of the age prior.

Figure 4 shows posterior distributions of the system age for two different age prior choices (uniform and log-flat). Both posteriors peak at 40–50 Myr but differ at the young and old extremes. The choice of prior significantly affects the old extreme of the posterior. However, under either prior, Columba’s age agrees well and BPMG’s is consistent (1.2 – 1.7σ).

Substellar cooling alone does not preclude older ages ($\gtrsim 100$ Myr), which have been shown to yield unstable orbits at the correspondingly higher masses ($> 12 M_{\text{Jup}}$). The high end of our mass posterior yields a smaller age peak at ≈ 200 Myr that corresponds to a resurgence in luminosity at older ages due to deuterium

fusion. Even though 9.8% of our dynamical mass posterior for HR 8799 e lies above $12 M_{\text{Jup}}$ (where deuterium burning is possible), the planets of the HR8799 system have not been considered deuterium-fusing objects, with masses below $\approx 13 M_{\text{Jup}}$, based on their luminosity and hypothesized youth (Marois et al. 2008; Marois et al. 2010). As well, they are unlikely to have masses in excess of $13 M_{\text{Jup}}$ on the basis of stability (Pueyo et al. 2015; Wang et al. 2018).

Excluding masses above $12 M_{\text{Jup}}$ yields an age distribution that is approximately Gaussian in $\log t$ for both priors (see dark-shaded posteriors in Figure 4). The resulting age posterior (under the log-flat prior) is $\log(t/\text{yr}) = 7.62 \pm 0.20$ dex (42^{+24}_{-16} Myr).

If the HR 8799 system is indeed a BPMG member, it would be coeval and perhaps co-compositional with the giant planets β Pic b and c that have dynamical masses of $9.3^{+2.6}_{-2.5} M_{\text{Jup}}$ and $8.3 \pm 1.0 M_{\text{Jup}}$, respectively (Brandt et al. 2021a). This cannot be ruled out by the dynamical masses. HR 8799 e and β Pic c have the same K -band absolute magnitude within the errors, 12.94 ± 0.02 mag and 12.9 ± 0.1 mag, respectively, and their masses are also consistent at 0.6σ .

The above discussion assumes that hot-start models are appropriate for deriving a substellar cooling age. If instead there was significant entropy loss in the formation of HR 8799 e, then it would be younger. Perhaps the initial entropy could even be tuned to match the age of the BPMG in a warm-start scenario. A younger age could also compensate for higher masses when considering the system’s long-term stability.

5. CONCLUSIONS

In this letter, we determine a dynamical mass for HR 8799 e of $9.6^{+1.9}_{-1.8} M_{\text{Jup}}$ by assuming that planets c, d and e share the same mass to within $\approx 20\%$. Marginalizing over a larger range of mass ratios for all four planets yields a dynamical mass of $9.4^{+2.2}_{-2.1} M_{\text{Jup}}$ for HR 8799 e. We favor the more precise mass for HR 8799 e given that the planets’ similar spectra and luminosities strongly suggest similar masses.

Our dynamical mass for HR 8799 e is $2 M_{\text{Jup}}$ (1.2σ) higher than previous estimates based on hot-start models (e.g., $7.2^{+0.6}_{-0.7} M_{\text{Jup}}$; Wang et al. 2018). We rule out, with 99.7% confidence, any planets with masses greater than $\approx 6 M_{\text{Jup}}$ and semi-major axes between ≈ 3 au and ≈ 8 au, as well as any additional $7 M_{\text{Jup}}$ or larger planets between 8 and 16 au.

We compute an updated bolometric luminosity for HR 8799 e and use hot-start evolutionary models to derive a substellar cooling age. We find 42^{+24}_{-16} Myr if we exclude the high-mass ($> 12 M_{\text{Jup}}$) portion of our mass

posterior, based on the low luminosity of HR 8799 e and the stability analysis of Wang et al. (2018). This is consistent with both the Columba association and β Pictoris moving group. Notably, the masses and absolute magnitudes of HR 8799 e and β Pic c are consistent within $<1\sigma$.

HR 8799 e, as the innermost planet on a ≈ 50 -year period, induces about 75% of the proper motion anomaly over the ≈ 25 -year *Hipparcos-Gaia* baseline. The uncertainty in our dynamical mass is dominated by the *Gaia* proper motion precision of HR 8799. Improved astrometric precision in future *Gaia* data releases will translate directly to improved mass measurements for the HR 8799 planets, especially for HR 8799 e and d.

Software: `astropy` (Astropy Collaboration et al. 2013; Price-Whelan et al. 2018), `scipy` (Virtanen et al. 2020), `numpy` (Oliphant 2006; van der Walt et al. 2011), `htof` (Brandt & Michalik 2020; Brandt et al. 2020, submitted), REBOUND (Rein & Liu 2012), Jupyter (<https://jupyter.org/>).

ACKNOWLEDGMENTS

G. M. B. is supported by the National Science Foundation (NSF) Graduate Research Fellowship under grant no. 1650114.

The orbits of the HR 8799 planets used in this work can be found at whereistheplanet.com. We thank Jason Wang, Matas Kulikauskas, and Sarah Blunt for building and hosting this wonderful web service, and for making their orbital posteriors open and freely available. We thank the anonymous referee for helpful comments that improved the quality of this work.

This work has made use of data from the European Space Agency (ESA) mission *Gaia* (<https://www.cosmos.esa.int/Gaia>), processed by the *Gaia* Data Processing and Analysis Consortium (DPAC, <https://www.cosmos.esa.int/web/Gaia/dpac/consortium>). Funding for the DPAC has been provided by national institutions, in particular the institutions participating in the *Gaia* Multilateral Agreement.

G.-D. M. acknowledges the support of the German Science Foundation (DFG) priority program SPP 1992 “Exploring the Diversity of Extrasolar Planets” (MA 9185/1-1). G.-D. M. acknowledges support from the Swiss National Science Foundation under grant BSSGI0_155816 “PlanetsInTime”. Parts of this work have been carried out within the framework of the NCCR PlanetS supported by the Swiss National Science Foundation.

This work made use of the `htof` code. We used version 0.3.4 (Brandt & Michalik 2020).

REFERENCES

- Astropy Collaboration, Robitaille, T. P., Tollerud, E. J., et al. 2013, *A&A*, 558, A33, doi: [10.1051/0004-6361/201322068](https://doi.org/10.1051/0004-6361/201322068)
- Bell, C. P. M., Mamajek, E. E., & Naylor, T. 2015, *MNRAS*, 454, 593, doi: [10.1093/mnras/stv1981](https://doi.org/10.1093/mnras/stv1981)
- Berardo, D., & Cumming, A. 2017, *ApJL*, 846, L17, doi: [10.3847/2041-8213/aa81c0](https://doi.org/10.3847/2041-8213/aa81c0)
- Berardo, D., Cumming, A., & Marleau, G.-D. 2017, *ApJ*, 834, 149, doi: [10.3847/1538-4357/834/2/149](https://doi.org/10.3847/1538-4357/834/2/149)
- Brandt, G. M., Brandt, T. D., Dupuy, T. J., Li, Y., & Michalik, D. 2021a, *AJ*, 161, 179, doi: [10.3847/1538-3881/abdc2e](https://doi.org/10.3847/1538-3881/abdc2e)
- Brandt, G. M., & Michalik, D. 2020, Zenodo, doi: [10.5281/zenodo.4118572](https://doi.org/10.5281/zenodo.4118572)
- Brandt, G. M., Michalik, D., Brandt, T. D., et al. 2020, submitted, *AJ*
- Brandt, T. D. 2018, *The Astrophysical Journal Supplement Series*, 239, 31, doi: [10.3847/1538-4365/aec06](https://doi.org/10.3847/1538-4365/aec06)
- . 2021, arXiv e-prints, arXiv:2105.11662, <https://arxiv.org/abs/2105.11662>
- Brandt, T. D., Dupuy, T. J., Li, Y., et al. 2021b, arXiv e-prints, arXiv:2105.11671, <https://arxiv.org/abs/2105.11671>
- Currie, T. 2016, arXiv e-prints, arXiv:1607.03980, <https://arxiv.org/abs/1607.03980>
- Currie, T., Burrows, A., Itoh, Y., et al. 2011, *ApJ*, 729, 128, doi: [10.1088/0004-637X/729/2/128](https://doi.org/10.1088/0004-637X/729/2/128)
- Dupuy, T. J., & Liu, M. C. 2017, *ApJS*, 231, 15, doi: [10.3847/1538-4365/aa5e4c](https://doi.org/10.3847/1538-4365/aa5e4c)
- ESA, ed. 1997, *The HIPPARCOS and TYCHO catalogues. Astrometric and photometric star catalogues derived from the ESA HIPPARCOS Space Astrometry Mission*, ESA Special Publication
- Esposito, S., Mesa, D., Skemer, A., et al. 2013, *A&A*, 549, A52, doi: [10.1051/0004-6361/201219212](https://doi.org/10.1051/0004-6361/201219212)

- Fabrycky, D. C., & Murray-Clay, R. A. 2010, *The Astrophysical Journal*, 710, 1408, doi: [10.1088/0004-637x/710/2/1408](https://doi.org/10.1088/0004-637x/710/2/1408)
- Filippazzo, J. C., Rice, E. L., Faherty, J., et al. 2015, *ApJ*, 810, 158, doi: [10.1088/0004-637X/810/2/158](https://doi.org/10.1088/0004-637X/810/2/158)
- Frantseva, K., Mueller, M., Pokorný, P., van der Tak, F. F. S., & ten Kate, I. L. 2020, *A&A*, 638, A50, doi: [10.1051/0004-6361/201936783](https://doi.org/10.1051/0004-6361/201936783)
- Gagné, J., Mamajek, E. E., Malo, L., et al. 2018, *ApJ*, 856, 23, doi: [10.3847/1538-4357/aaae09](https://doi.org/10.3847/1538-4357/aaae09)
- Gaia Collaboration, Brown, A. G. A., Vallenari, A., et al. 2020, arXiv e-prints, arXiv:2012.01533. <https://arxiv.org/abs/2012.01533>
- Gaia Collaboration, Prusti, T., de Bruijne, J. H. J., et al. 2016, *A&A*, 595, A1, doi: [10.1051/0004-6361/201629272](https://doi.org/10.1051/0004-6361/201629272)
- Götberg, Y., Davies, M. B., Mustill, A. J., Johansen, A., & Church, R. P. 2016, *A&A*, 592, A147, doi: [10.1051/0004-6361/201526309](https://doi.org/10.1051/0004-6361/201526309)
- Goździewski, K., & Migaszewski, C. 2018, *ApJS*, 238, 6, doi: [10.3847/1538-4365/aad3d3](https://doi.org/10.3847/1538-4365/aad3d3)
- . 2020, *ApJL*, 902, L40, doi: [10.3847/2041-8213/abb881](https://doi.org/10.3847/2041-8213/abb881)
- Gravity Collaboration, Lacour, S., Nowak, M., et al. 2019, *A&A*, 623, L11, doi: [10.1051/0004-6361/201935253](https://doi.org/10.1051/0004-6361/201935253)
- Konopacky, Q. M., Marois, C., Macintosh, B. A., et al. 2016, *AJ*, 152, 28, doi: [10.3847/0004-6256/152/2/28](https://doi.org/10.3847/0004-6256/152/2/28)
- Lee, J., & Song, I. 2019, *MNRAS*, 489, 2189, doi: [10.1093/mnras/stz2290](https://doi.org/10.1093/mnras/stz2290)
- Lindgren, L., Hernandez, J., Bombrun, A., et al. 2018, arXiv. <https://arxiv.org/abs/1804.09366>
- Lindgren, L., Klioner, S. A., Hernández, J., et al. 2020, arXiv e-prints, arXiv:2012.03380. <https://arxiv.org/abs/2012.03380>
- Marleau, G. D., & Cumming, A. 2014, *MNRAS*, 437, 1378, doi: [10.1093/mnras/stt1967](https://doi.org/10.1093/mnras/stt1967)
- Marleau, G.-D., Mordasini, C., & Kuiper, R. 2019, *ApJ*, 881, 144, doi: [10.3847/1538-4357/ab245b](https://doi.org/10.3847/1538-4357/ab245b)
- Marley, M. S., Fortney, J. J., Hubickyj, O., Bodenheimer, P., & Lissauer, J. J. 2007, *ApJ*, 655, 541, doi: [10.1086/509759](https://doi.org/10.1086/509759)
- Marois, C., Macintosh, B., Barman, T., et al. 2008, *Science*, 322, 1348, doi: [10.1126/science.1166585](https://doi.org/10.1126/science.1166585)
- Marois, C., Zuckerman, B., Konopacky, Q. M., Macintosh, B., & Barman, T. 2010, *Nature*, 468, 1080, doi: [10.1038/nature09684](https://doi.org/10.1038/nature09684)
- Mollière, P., Stolker, T., Lacour, S., et al. 2020, *A&A*, 640, A131, doi: [10.1051/0004-6361/202038325](https://doi.org/10.1051/0004-6361/202038325)
- Oliphant, T. 2006, *NumPy: A guide to NumPy, USA*: Trelgol Publishing. <http://www.numpy.org/>
- Price-Whelan, A. M., Sipőcz, B. M., Günther, H. M., et al. 2018, *AJ*, 156, 123, doi: [10.3847/1538-3881/aabc4f](https://doi.org/10.3847/1538-3881/aabc4f)
- Pueyo, L., Soummer, R., Hoffmann, J., et al. 2015, *ApJ*, 803, 31, doi: [10.1088/0004-637X/803/1/31](https://doi.org/10.1088/0004-637X/803/1/31)
- Rein, H., & Liu, S. F. 2012, *A&A*, 537, A128, doi: [10.1051/0004-6361/201118085](https://doi.org/10.1051/0004-6361/201118085)
- Rein, H., & Spiegel, D. S. 2015, *MNRAS*, 446, 1424, doi: [10.1093/mnras/stu2164](https://doi.org/10.1093/mnras/stu2164)
- Saumon, D., & Marley, M. S. 2008, *ApJ*, 689, 1327, doi: [10.1086/592734](https://doi.org/10.1086/592734)
- Spiegel, D. S., Burrows, A., & Milsom, J. A. 2011, *ApJ*, 727, 57, doi: [10.1088/0004-637X/727/1/57](https://doi.org/10.1088/0004-637X/727/1/57)
- Sudol, J. J., & Haghighipour, N. 2012, *ApJ*, 755, 38, doi: [10.1088/0004-637X/755/1/38](https://doi.org/10.1088/0004-637X/755/1/38)
- van der Walt, S., Colbert, S. C., & Varoquaux, G. 2011, *Computing in Science and Engineering*, 13, 22, doi: [10.1109/MCSE.2011.37](https://doi.org/10.1109/MCSE.2011.37)
- van Leeuwen, F. 2007, *A&A*, 474, 653, doi: [10.1051/0004-6361:20078357](https://doi.org/10.1051/0004-6361:20078357)
- Virtanen, P., Gommers, R., Oliphant, T. E., et al. 2020, *Nature Methods*, 17, 261, doi: <https://doi.org/10.1038/s41592-019-0686-2>
- Wahhaj, Z., Milli, J., Romero, C., et al. 2021, arXiv e-prints, arXiv:2101.08268. <https://arxiv.org/abs/2101.08268>
- Wang, J., Wang, J. J., Ma, B., et al. 2020, *AJ*, 160, 150, doi: [10.3847/1538-3881/ababa7](https://doi.org/10.3847/1538-3881/ababa7)
- Wang, J. J., Kulikaukas, M., & Blunt, S. 2021, whereistheplanet: Predicting positions of directly imaged companions. <http://ascl.net/2101.003>
- Wang, J. J., Graham, J. R., Dawson, R., et al. 2018, *AJ*, 156, 192, doi: [10.3847/1538-3881/aae150](https://doi.org/10.3847/1538-3881/aae150)
- Zuckerman, B., Rhee, J. H., Song, I., & Bessell, M. S. 2011, *ApJ*, 732, 61, doi: [10.1088/0004-637X/732/2/61](https://doi.org/10.1088/0004-637X/732/2/61)